J Pharmacol Sci **92**, 115 – 123 (2003)

Journal of Pharmacological Sciences

Full Paper

Involvement of Wiskott-Aldrich Syndrome Protein Family Verprolin-Homologous Protein (WAVE) and Rac1 in the Phagocytosis of Amyloid-β(1 – 42) in Rat Microglia

Yoshihisa Kitamura[1,†], Keiichi Shibagaki[1,†], Kazuyuki Takata[1], Daiju Tsuchiya[1], Takashi Taniguchi[1], Peter J. Gebicke-Haerter[2], Hiroaki Miki[3], Tadaomi Takenawa[3], and Shun Shimohama[4,*]

[1]*Department of Neurobiology, Kyoto Pharmaceutical University, Kyoto 607-8412, Japan*
[2]*Department of Psychopharmacology, Central Institute of Mental Health, Mannheim 68159, Germany*
[3]*Division of Cancer Genomics, Institute of Medical Science, University of Tokyo, Tokyo 108-8639, Japan*
[4]*Department of Neurology, Graduate School of Medicine, Kyoto University, Kyoto 606-8507, Japan*

Received January 27, 2003; Accepted March 11, 2003

Abstract. Alzheimer's disease (AD) is characterized by the accumulation of extracellular amyloid-β (Aβ) fibrils with microglia. Recently, there has been great interest in the microglial phagocytosis of Aβ, because the microglial pathway is considered to be one of the Aβ clearance pathways in the brain parenchyma. However, the mechanism of microglial phagocytosis of Aβ is not fully understood and, thus, was investigated in this study. At one minute after exposure to Aβ(1 – 42) (Aβ42), Aβ immunoreactivity was detected at the cell surface of microglia. After 1 h, marked immunoreactivity was observed in the cytosolic vesicles. At 12 h, delayed phagocytosis of fibrillar Aβ42 was also observed with the formation of a large phagocytic cup. The microglial cell shape rapidly changed to an ameboid form during the process of phagocytosis. Although neither neural Wiskott-Aldrich syndrome protein (N-WASP) nor WASP interacting SH3 protein (WISH) immunoreactivity was co-localized with filamentous actin (F-actin) distribution, both WASP family verprolin-homologous protein (WAVE) and Rac1 immunoreactivity was co-localized with F-actin in the lamellipodia of phogocytic microglia. These results suggest that WAVE and Rac1 participate in the phagocytosis of Aβ42 by microglia.

Keywords: Wiskott-Aldrich syndrome protein family verprolin-homologous protein (WAVE), Rac1, amyloid-β(1 – 42), microglial phagocytosis, Alzheimer's disease

Introduction

One of the pathological characteristics of Alzheimer's disease (AD) is the formation of extracellular senile plaques associated with activated microglia (1 – 3). Epidemiological studies have shown that a reduction in AD prevalence occurs among users of non-steroidal anti-inflammatory drugs (NSAIDs) (4). Microglial activation has also been found to be intimately involved in inflammatory responses in AD brains (3). However, the pathogenesis of microglial activation in this disease has not been clarified. Conversely, it has been reported that glial cells support neuronal function and that microglial activation also induces the production of neurotrophic factors (5). In the brains of double transgenic mice carrying both mutant presenilin-1 and Aβ precursor protein transgenes (PS/APP mouse), high levels of amyloid-β (Aβ) peptides were produced and reactive microglia accumulated around the Aβ deposits (6). However, global neuronal loss was not detected (7). In addition, a nitric oxide-releasing NSAID, NCX-2216, dramatically reduced Aβ deposits with an increase in activated microglia in PS/APP mice (8). Based on these observations, it is likely that microglial activation does not directly cause the exacerbation of neurodegeneration, but it appears that microglia act as sensors of pathological events in the brain (9).

There have been controversial reports that microglia

[†]The first two authors equally contributed to this study.
*Corresponding author. FAX: +81-75-751-3265
E-mail: i53367@sakura.kudpc.kyoto-u.ac.jp

drive plaque formation (10, 11) and that microglia phagocytose Aβ peptides (12 – 14). Recent studies have suggested that antibodies to Aβ, produced by Aβ immunotherapy (15), induce microglial phagocytosis (16), and/or sequester plasma Aβ peptides (17). Transforming growth factor β1 (TGF-β1), produced by astrocytes, may participate in microglial Aβ clearance (18). We recently reported that extracellular Aβ(1 – 42) peptide (Aβ42), rather than Aβ(1 – 40), was markedly phagocytosed by rat microglia after exposure. Maximal phagocytosis of Aβ42 occurred at 12 h after exposure and then gradually decreased, as assessed by immunoblot analysis using anti-Aβ antibody (19, 20). In addition, insulin or pepstatin A, but not phosphoramidon (neprilysin inhibitor), suppressed the decrease in Aβ42 levels in microglia after 72 h. This suggests that phagocytosed Aβ42 is degraded by an insulin-degrading enzyme (IDE)-like peptidase and/or cathepsin D-like aspartic proteinase in rat microglia (20). However, the mechanism of microglial phagocytosis of Aβ peptides has not been elucidated.

It has been reported that morphogenesis, cell movement, and phagocytosis are driven by dynamic reorganization of the actin cytoskeleton (21, 22). Small GTPases in the Ras-homologous (Rho) family, such as cell-division cycle 42 protein (Cdc42) and Ras-related C3 botulinum toxin substrate 1 (Rac1), were shown to induce filopodium and lamellipodium formation (23). Recently, the neural Wiskott-Aldrich syndrome protein (N-WASP) and WASP family verprolin-homologous protein (WAVE) have been identified as key molecules participating specifically in filopodium and lamellipodium formation through Cdc42 and Rac1, respectively (24 – 26). In addition, N-WASP-induced formation of filopodia was facilitated by WASP interacting SH3 protein (WISH) in a Cdc42-independent manner (27). In the present study, we examined changes in the distribution of filamentous actin (F-actin), WAVE, Rac1, N-WASP, WISH, and Cdc42, during the process of microglial phagocytosis of Aβ42.

Materials and Methods

Materials

The hydrochloride (HCl) form of Aβ42, rhodamine-conjugated phalloidin and cytochalasin D were purchased from AnaSpec (San Jose, CA, USA), Molecular Probes (Eugene, OR, USA) and Sigma (St. Louis, MO, USA), respectively. Antibodies against N-WASP and WISH were prepared as described previously (27, 28). Other primary antibodies included rabbit polyclonal anti-WAVE antibody (Santa Cruz Biotechnology, Santa Cruz, CA, USA) and mouse monoclonal antibodies to Aβ (Chemicon, Temecula, CA, USA), Rac1 (BD Transduction Laboratories, Lexington, KY, USA), and Cdc42 (Santa Cruz Biotechnology). The enhanced chemiluminescent detection system kit (ECL kit) from Amersham Pharmacia Biotech (Buckinghamshire, UK) and Bradford protein assay from BioRad Laboratories (Hercules, CA, USA) were used.

Microglial culture

Mixed glial cells (a mixture of astrocytes and microglia) were prepared from the cerebral hemispheres, which were carefully removed from the meninges of newborn Wistar rats (SLC, Inc., Shizuoka). The tissue suspension was filtered through a 50-μm-diameter nylon mesh (cell strainers; Falcon, Franklin Lakes, NJ, USA) into 50 ml tubes and cells were collected by centrifugation at $200 \times g$ for 10 min. Cells were resuspended in Dulbecco's modified Eagle's medium supplemented with 10% fetal calf serum, plated out into 100-mm-diameter dishes and incubated at 37°C in 5% CO_2/95% air. Floating microglia were harvested from mixed glial cultures and plated out into new culture dishes, taking extreme care to avoid contamination by endotoxins (20, 29).

Cell treatment, laser confocal analysis and quantitative analysis

In our experiments, the HCl form of Aβ42, which aggregates more readily than the trifluoroacetic acid form (30), was used. Although the microglia had an ameboid type shape immediately after attachment to new culture dishes, the cell shapes gradually resumed the resting ramified form. Therefore, we used microglia after at least 10 h incubation in new dishes. Rat microglia (over 97% pure) were treated with vehicle or 3 μM Aβ42 in the presence or absence of cytochalasin D. After treatment, the cells were gently washed with PBS for 3 times and then fixed. Cells were incubated with primary antibody against Aβ, WAVE, Rac1, N-WASP, WISH, or Cdc42 (each diluted 1:1000), followed by the appropriate secondary antibody linked to fluorescein isothiocyanate (FITC). Rhodamine-conjugated phalloidin was used to visualize actin filaments. The fluorescence and cellular images (the difference interference contrast, DIC) were observed using a laser scanning confocal microscope LSM410 (Carl Zeiss, Jena, Germany).

For the semi-quantitative analysis, images of Aβ immunoreactivity in microglia were scanned using a laser scanning confocal microscope LSM410 and then analyzed (WinRoof; Mitani, Fukui) (31). The Aβ-immunoreactive areas in the cytosolic (inner space of phalloidin-staining) region and the cell surface (double staining of phalloidin and anti-Aβ antibody) region and

total Aβ-immunoreactive area were measured (μm^2).

Immunoblotting and semi-quantitative analysis

After treatment with vehicle or Aβ42 in the presence or absence of cytochalasin D, microglia were washed with phosphate-buffered saline (PBS) and then collected and lysed. Aliquots containing 10 μg of protein were analyzed by sodium dodecyl sulfate-polyacrylamide gel electrophoresis (SDS-PAGE) and then transferred to a polyvinylidene difluoride (PVDF) membrane (BioRad). The PVDF membrane was incubated with Tris-buffered saline (pH 7.4) containing 0.3% Triton X-100 (TBS-T) and 5% dehydrated skimmed milk (Difco Laboratories, Detroit, MI, USA) to block nonspecific protein binding. The membrane was then incubated with antibody to Aβ (1:3000), WAVE (1:1000), Rac1 (1:1000), N-WASP (1:1000), WISH (1:5000), or Cdc42 (1:100), followed by secondary antibody, horseradish peroxidase (HRP)-linked antibodies against either rabbit or mouse immunoglobulin (each diluted 1:1000). Subsequently, bound HRP-labeled antibodies were detected by chemiluminescence (ECL kit). The protein bands that reacted with the antibodies were detected on radiographic film (X-Omat JB-1; Kodak, Rochester, NY, USA) 5 – 60 s after exposure.

For semi-quantitative analysis, the bands of these proteins on radiographic films were scanned with a CCD color scanner (DuoScan; AGFA, Leverkusen, Germany) and then analyzed. Densitometric analysis was performed using the public domain NIH Image 1.56 program (written by Wayne Rasband at the U.S. National Institutes of Health and available from the Internet by anonymous ftp from zippy.nimh.nih.gov.).

Statistical evaluation

Results from the confocal analysis of immunoreactive images and the densitometric analysis of immunoblots are given as the mean ± standard error of the mean (S.E.M.). The statistical significance of differences was determined by analysis of variance (ANOVA). Further statistical analysis for *post hoc* comparisons was carried out using the Bonferroni/Dunn test.

Results

Aβ42-induced membrane ruffling and its phagocytosis by rat microglia

Until Aβ42 attached to the cell surface, the microglia had a ramified resting shape of a slender cell body with some processes (Fig. 1A). After 1 min, slight Aβ immunoreactivity was detected at the microglial cell surface and was partially co-localized with F-actin (Fig. 1B). Subsequently, the microglia formed a rounded up ameboid cell body with lamellipodia, and phalloidin-stained retraction fibers were observed in the cell periphery (Fig. 1: C – E). In addition, pitted bundles of F-actin with Aβ peptides were observed like small phagocytic cups after 5 min (Fig. 1: C, D). After 1 h, marked Aβ immunoreactivity was detected in the cytosolic vesicles (Fig. 1: E – G). Thus, Aβ42 may rapidly induce actin reorganization to cause ameboid shaped microglia with lamellipodia and is then taken up into cytosolic vesicles. We measured the Aβ-immunoreactive areas in the cell surface (membrane) region and the cytosolic region and the total Aβ-immunoreactive area (Fig. 1H). On the microglial cell surface, Aβ immunoreactivity was increased within 5 min and then gradually enhanced. On the other hand, the cytosolic Aβ immunoreactivity was markedly increased after 30 min (Fig. 1H).

Since we used the HCl form of Aβ42 that readily forms the β-sheet structure itself (30), the fibril-like structure of Aβ42 was observed to some extent in microglial culture (Fig. 2). In this case, the microglia migrated and associated with the Aβ42 fibrils (Fig. 2A), which they attempted to phagocytose (Fig. 2: B, C). Later (at 12 h), a large circular bundle of F-actin surrounding fibrillar Aβ formed a large phagocytic cup and Aβ immunoreactivity was also detected in cytosolic vesicles (Fig. 2D).

Cytochalasin D-induced inhibition of Aβ42 phagocytosis in rat microglia

To clarify the relationship between the actin assembly and the phagocytosis of Aβ42 in rat microglia, we examined the effect of cytochalasin D, an inhibitor of actin assembly (32). After the pre-incubation for 30 min with cytochalasin D, Aβ42 was added into the microglial culture, and then we assessed the total amount of Aβ42 in microglia (membrane-bound and phagocytosed Aβ42) by immunoblot assay using anti-Aβ antibody (Fig. 3: A, B). After 24 h, the amount of Aβ42 in the microglia was inhibited by cytochalasin D in a concentration-dependent manner. Similarly, total Aβ-immunoreactive area in the microglia after 3 h was suppressed by 3 μM cytochalasin D (Fig. 3: C, D). In brief, cytochalasin D markedly reduced the cytosolic Aβ-immunoreactive area, but it significantly increased membrane-bound Aβ-immunoreactivity (Fig. 3: C, D). Thus, an inhibition of actin assembly causes the suppression in microglial phagocytosis of Aβ42 and the accumulation of extracellular Aβ42.

Alteration in the distribution of WAVE and Rac1 during the phagocytosis of Aβ42 in rat microglia

Normal microglia formed a ramified shape with slight formation of lamellipodium- and filopodium-like struc-

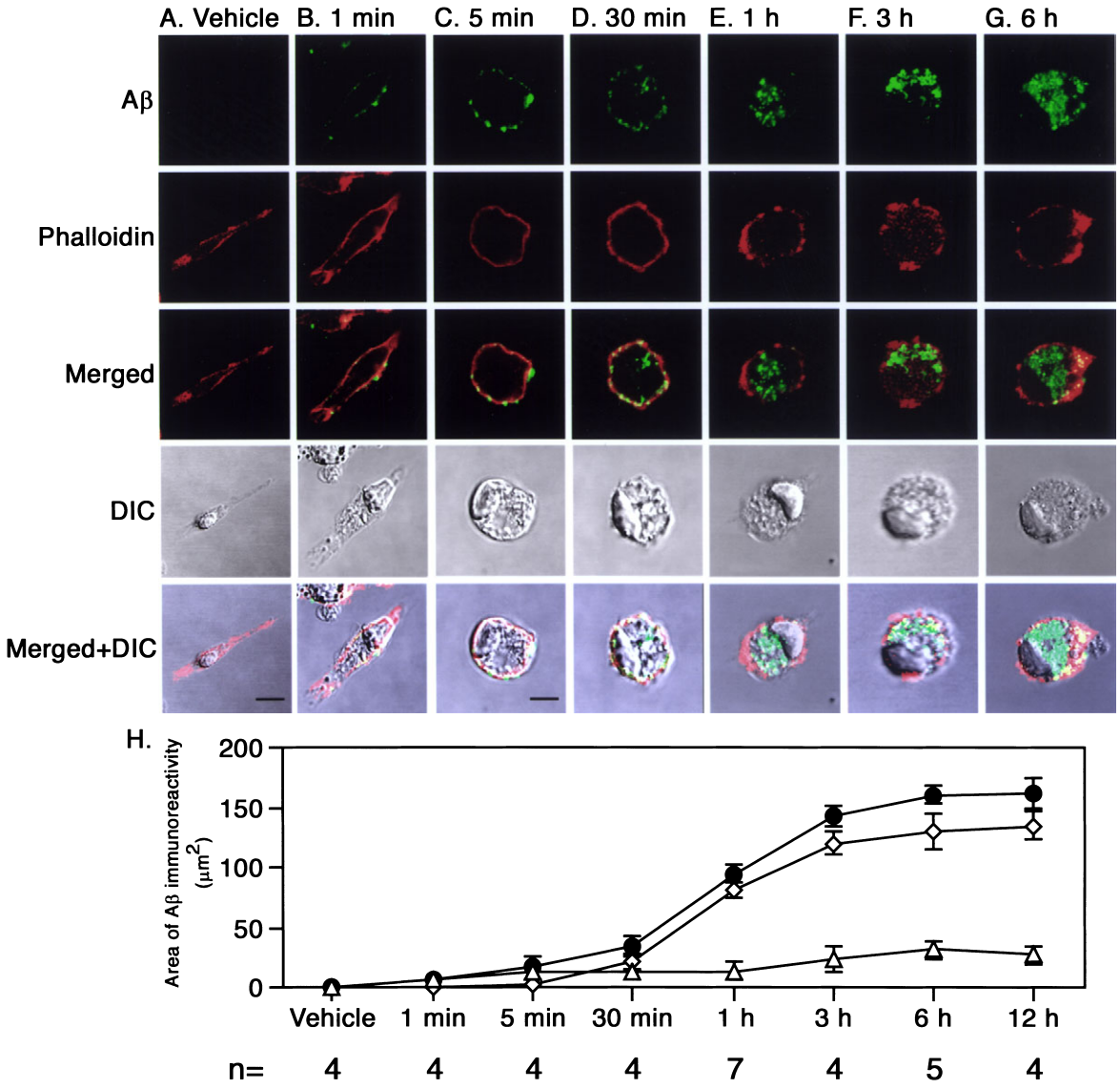

Fig. 1. Morphological changes and phagocytosis of Aβ42 in rat microglia. Rat microglia were treated with 3 μM Aβ42 for 1 min (B), 5 min (C), 30 min (D), 1 h (E), 3 h (F), and 6 h (G). The control was treated for 1 h with vehicle in the absence of Aβ42 (A). After treatment, cells were washed and fixed. Subsequently, confocal analysis was performed using anti-Aβ antibody (green, first panels) and rhodamine-conjugated phalloidin (red, second panels). The merged images are shown in the third panels. Images of cell shapes (DIC, fourth panels) were also obtained using confocal laser microscopy. In addition, fifth panels are the overlay of merged colors and DIC. Scale bars, 15 μm (for A and B); 10 μm (for C – G). H: Time-dependent changes in the Aβ-immunoreactive areas in the cell surface region (open triangle) and the cytosolic region (open diamond), and the total Aβ-immunoreactive area (closed circle) after Aβ42 exposure. n, the number of microglia measured Aβ-immunoreactive areas.

tures at the cell edges (Fig. 4). In these cells, phalloidin-labeled F-actin was detected predominantly in the substratum and showed a slight punctate distribution in the cytoplasm. Marked WAVE immunoreactivity was observed in the cytoplasm and, to a lesser extent, in lamellipodium-like structures where it was partially co-localized with F-actin (Fig. 4A). A similar distribution was observed for Rac1 immunoreactivity in control microglia (Fig. 4B). N-WASP, WISH, and Cdc42 immunoreactivity was predominantly detected in the cytoplasm showing partial co-localization with F-actin (Fig. 4: C – E).

At 1 h after treatment with 3 μM Aβ42, resting microglia transformed into an ameboid shape, which showed retracted processes and an enlarged cell body (Figs. 1E and 5). Aβ immunoreactivity was detected in the cytosolic vesicles in these cells (Fig. 1E). At this time, WAVE and Rac1 immunoreactivity was almost com-

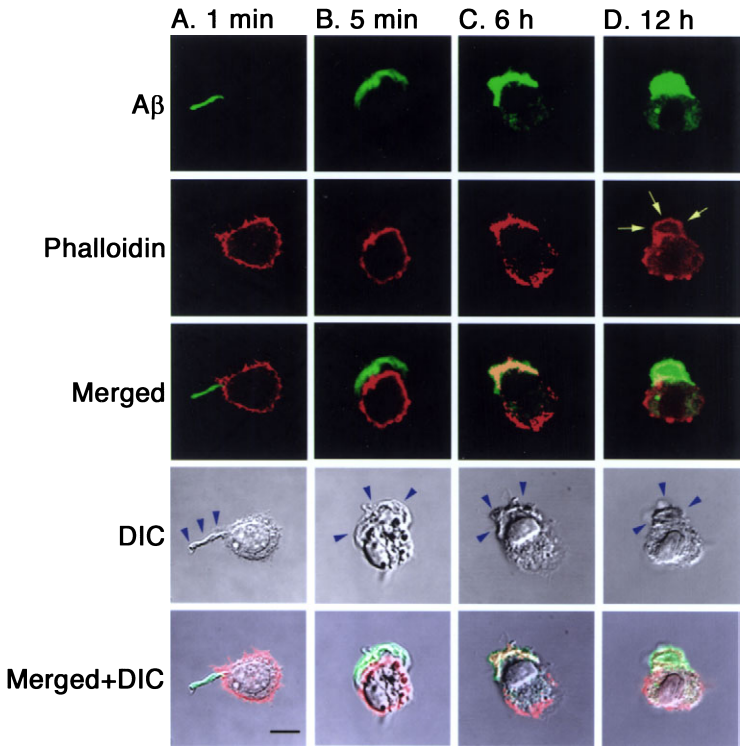

Fig. 2. Phagocytosis of fibrillar Aβ42 in rat microglia. Rat microglia were treated with 3 μM Aβ42 for 1 min (A), 5 min (B), 6 h (C), and 12 h (D). After treatment, cells were washed and fixed. Subsequently, confocal analysis was performed using anti-Aβ antibody (green) and phalloidin (red). Arrowheads (blue) and arrows (yellow) indicate the fibril-like structure of Aβ42 (A – D, DIC) and a large phagocytic cup (D, phalloidin), respectively. Scale bar, 10 μm (for A – D).

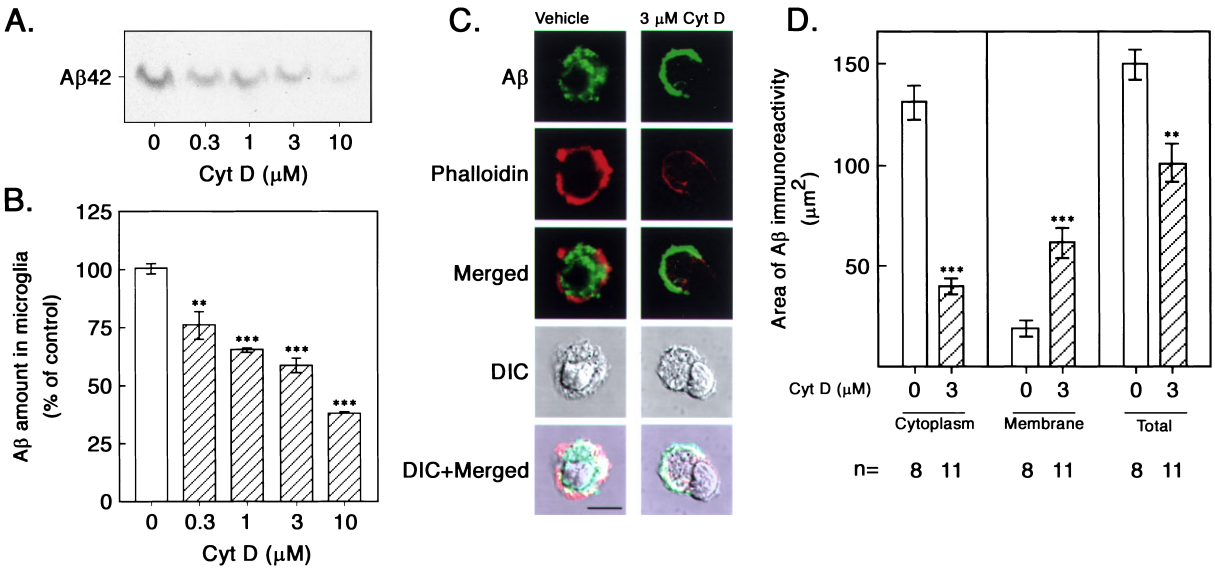

Fig. 3. Inhibitory effect of cytochalasin D on the Aβ42 phagocytosis by microglia. Rat microglia were treated for 24 h (A, B) or 3 h (C, D) with vehicle or Aβ42 at 0.3 μM (A, B) or 3 μM (C, D) in the presence or absence of cytochalasin D (Cyt D) at 0 – 10 μM. A and B: After treatment for 24 h, cells were washed and lysed, and then immunoblotted with anti-Aβ antibody. The density of the protein band in the vehicle treatment (at 0 μM) was taken as 100%. Each value is the mean ± S.E.M. of 3 determinations. C and D: After treatment for 3 h, cells were washed and fixed. Subsequently, confocal analysis was performed using anti-Aβ antibody (green) and phalloidin (red). Scale bar, 10 μm (C). In addition, Aβ-immunoreactive areas in the cytosolic region (Cytoplasm) and the cell surface region (Membrane) and the total Aβ-immunoreactive area (Total) were measured. Each value is the mean ± S.E.M. of 8 cells of vehicle control microglia and 11 cells of microglia treated with 3 μM cytochalasin D. $^{**}P<0.01$; $^{***}P<0.001$ vs the vehicle control (at 0 μM).

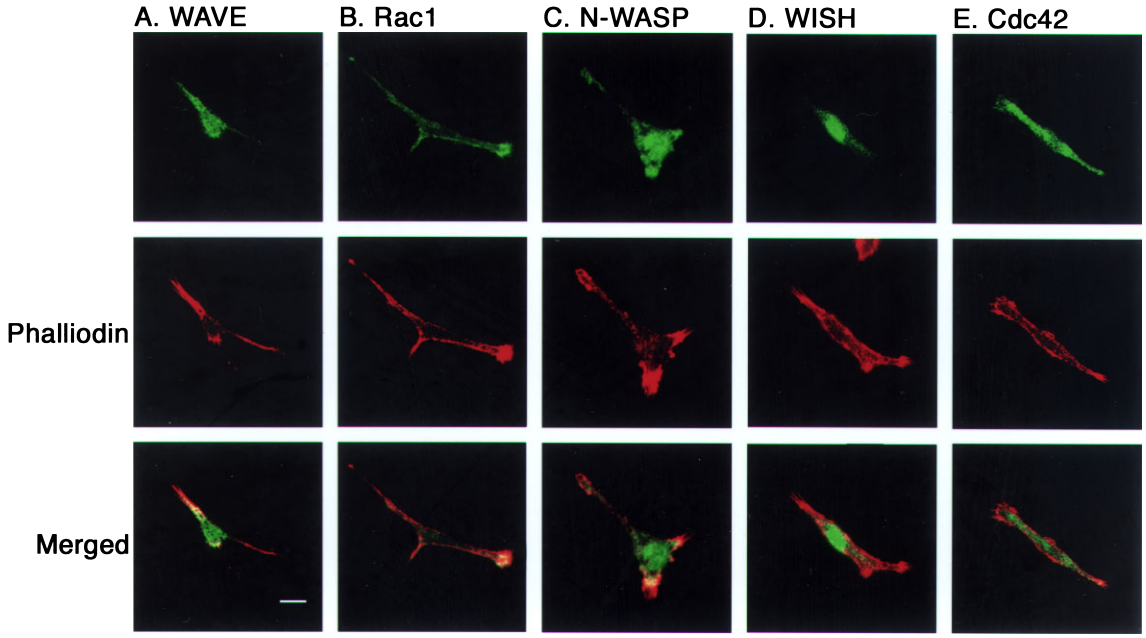

Fig. 4. Localization of WAVE, Rac1, N-WASP, WISH, and Cdc42 in resting microglia. Microglia were treated for 1 h with vehicle alone. After treatment, cells were washed and fixed. Subsequently, confocal analysis was performed using antibody (green, upper panels) against WAVE (A), Rac1 (B), N-WASP (C), WISH (D), or Cdc42 (E), and rhodamine-conjugated phalloidin (red, middle panels). The merged images are shown in the lower panels. Scale bar, 15 μm (for A – E).

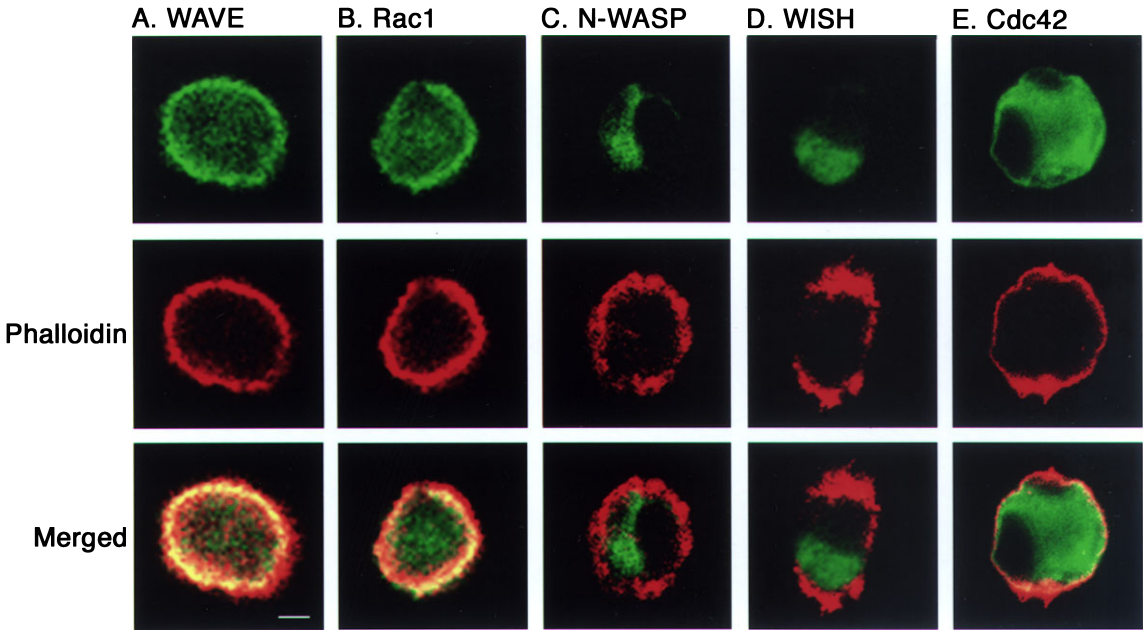

Fig. 5. Localization of WAVE, Rac1, N-WASP, WISH, and Cdc42 in phagocytic ameboid microglia. Microglia were treated for 1 h with 3 μM Aβ42. After treatment, cells were washed and fixed. Subsequently, confocal analysis was performed using antibody (green, upper panels) against WAVE (A), Rac1 (B), N-WASP (C), WISH (D), or Cdc42 (E), and rhodamine-conjugated phalloidin (red, middle panels). These merged images were shown in lower panels. Notes: WAVE and Rac1 immunoreactivity was overlapped with phalloidin-labeled F-actin in the lamellipodia. Scale bar, 4 μm (for A – E).

pletely co-localized with phalloidin-labeled F-actin in the lamellipodia and in a punctate distribution in the cytoplasm (Fig. 5: A, B). N-WASP and WISH immunoreactivity was not co-localized with phalloidin fluores-

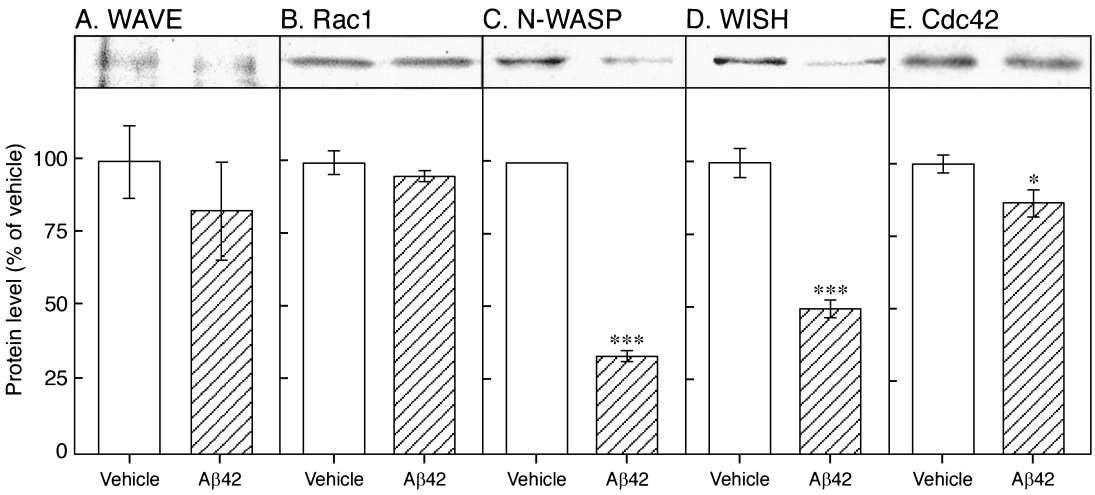

Fig. 6. Changes in protein levels of WAVE, Rac1, N-WASP, WISH, and Cdc42 in microglia. Microglia were treated for 1 h with vehicle or 3 μM Aβ42. Subsequently, cells were washed and lysed. Each sample (10 μg protein/lane) was subjected to immunoblot analysis of antibodies against WAVE (A), Rac1 (B), N-WASP (C), WISH (D), and Cdc42 (E). 80-kDa WAVE, 21-kDa Rac1, 65-kDa N-WASP, 90-kDa WISH, and 25-kDa Cdc42 were detected in each immunoblot of cell lysates (upper panels). The density of protein band in the vehicle treatment was taken as 100%. Each value is the mean ± S.E.M. of 6 determinations. *P<0.05. ***P<0.001 vs the vehicle control.

cence (Fig. 5: C, D), but Cdc42 immunoreactivity was partially co-localized with F-actin in the substratum (Fig. 5E).

We further examined the levels of these proteins after treatment with Aβ42. In immunoblots of rat microglial cell lysates, the molecular masses of WAVE, Rac1, N-WASP, WISH, and Cdc42 were approximately 80-, 21-, 65-, 90-, and 25-kDa, respectively. The protein levels of WAVE and Rac1 did not change, even after treatment with Aβ42 (Fig. 6: A, B). Conversely, protein levels of N-WASP and WISH were markedly reduced (Fig. 6: C, D), and the Cdc42 level was slightly decreased (Fig. 6E).

Discussion

Recently, there has been great interest in the microglial phagocytosis of Aβ, because microglia are thought to clear Aβ42 from the brain parenchyma (16, 18, 20). In the present study, we clearly showed that exposure of cultured rat microglia to Aβ42 induced morphological changes from the resting form to the ameboid type (reactive form). Microglia rapidly phagocytosed soluble or small particle-like Aβ42 peptides. In addition, an inhibitor of actin assembly, cytochalasin D, significantly reduced Aβ42 phagocytosis. On the other hand, since Aβ immunoreactivity was detected in cytosolic vesicles at 12 h, after the association with Aβ42 fibrils, rat microglia are able, at least partially, to phagocytose fibrillar Aβ42. However, it is possible that other extracellular Aβ42 peptides, such as monomers and small oligomers, were simultaneously phagocytosed by microglia.

Recently, WAVE and N-WASP/WISH were identified as critical regulators in the formation of lamellipodia and filopodia in the co-author's laboratory (24, 27, 33, 34). WAVE regulates the formation of membrane ruffles and lamellipodia by activating the actin-related protein 2/3 (Arp2/3) complex downstream of Rac1 (25, 26, 34). N-WASP-induced formation of filopodia is mediated in a Cdc42- or WISH-dependent manner (24, 26, 27, 33). In the present study, WAVE and Rac1 immunoreactivity was partially co-localized with F-actin in resting microglia and almost completely co-localized with F-actin in the lamellipodia of ameboid microglia. In contrast, neither N-WASP nor WISH immunoreactivity co-localized with F-actin in ameboid microglia. Although the protein levels of WAVE and Rac1 were not changed, levels of N-WASP and WISH were markedly reduced after exposure to Aβ42. Thus, it appears that N-WASP and WISH may not participate in the microglial phagocytosis of Aβ42.

Although stress fibers and associated focal adhesions are absent in hematopoietic cells, small focal complexes were detected in the mouse macrophage cell line Bac1.2F5 (35). These complexes, which are distinct from Rho-induced focal adhesions, are associated with lamellipodia and filopodia through Rac1 and Cdc42, and contain vinculin, paxillin, focal adhesion kinase, and β3 integrin (36). Recent reports indicated that over-

expression of the dominant negative Rac1 mutant, N17Rac1, inhibited lamellipodium formation and membrane ruffling in Bac1.2F5 macrophages (35) and membrane ruffling and phagocytic cup formation in the mouse MG5 microglial cell line (22). These results suggest that Rac1 predominantly participates in the formation of membrane ruffles, lamellipodia, and phagocytic cups in mouse macrophages and microglia. Interestingly, dominant negative N17Cdc42 slightly inhibited the formation of focal complexes in Bac1.2F5 macrophages and of phagocytic cups in MG5 microglia (22, 35). Therefore, it is possible that Cdc42 may act, in part, upstream of Rac1 to regulate the formation of focal complexes and phagocytic cups in macrophages and microglia (22, 35). In our present study, Cdc42 immunoreactivity, but not that of N-WASP or WISH, was partially co-localized with F-actin in the microglial cytoplasm. Although the protein levels of N-WASP and WISH were markedly decreased after Aβ42 exposure, the Cdc42 level was only slightly reduced. Thus, the Cdc42 profile is more similar to those of WAVE and Rac1, than to those of N-WASP and WISH. From these observations, we presume that Rac1 and WAVE, rather than WISH and N-WASP, participate in the morphological changes in microglia and in their phagocytosis of Aβ42. Cdc42 may also contribute, in part, to the formation of lamellipodia in rat microglia. Despite recent setbacks in the human clinical phase IIa trials of Aβ vaccination (37), its experimental effectiveness in preventing plaque development in Aβ deposit-forming transgenic mice models of AD indicates that further investigations are warranted (8, 15, 16, 38). Therefore, microglial clearance of Aβ42 may be another option to investigate in the search for a therapeutic strategy for AD.

In conclusion, Aβ immunoreactivity was detected at the cell surface of microglia at 1 min after exposure to Aβ42. After 1 h, marked immunoreactivity was observed in the cytosolic vesicles. Interestingly, delayed phagocytosis of fibrillar Aβ42 was also observed with the formation of a large phagocytic cup. During the process of microglial phagocytosis, the cell shape rapidly changed to an ameboid form. Although neither N-WASP nor WISH immunoreactivity was co-localized with F-actin, WAVE, and Rac1 immunoreactivity was co-localized with F-actin in the lamellipodium of ameboid microglia. These results suggest that WAVE and Rac1 may predominantly participate in the phagocytosis of Aβ42 in microglia.

Acknowledgments

This study was supported in part by a Frontier Research Program (T. Taniguchi), Grants-in-Aid from the Ministry of Education, Culture, Sports, Science, and Technology of Japan (Y.K., T. Taniguchi, H.M., T. Takenawa, S.S.) and a Grant-in-Aid for the promotion of the advancement of education and research in graduate schools (Special Research) from the Promotion and Mutual Aid Corporation for Private Schools of Japan (T. Taniguchi).

References

1 Selkoe DJ. Translating cell biology into therapeutic advances in Alzheimer's disease. Nature. 1999;399 Suppl:A23–A31.
2 Kitamura Y, Taniguchi T, Shimohama S. Apoptotic cell death in neurons and glial cells: implications for Alzheimer's disease. Jpn J Pharmacol. 1999;79:1–5.
3 Neuroinflammation working group: Akiyama H, Barger S, Barnum S, et al. Inflammation and Alzheimer's disease. Neurobiol Aging. 2000;21:383–421.
4 in t' Veld BA, Ruitenberg A, Hofman A, et al. Nonsteroidal antiinflammatory drugs and the risk of Alzheimer's disease. N Engl J Med. 2001;345:1515–1521.
5 Kettenmann H, Ransom BR, editors. Neuroglia. New York and Oxford: Oxford University Press; 1995.
6 Holcomb L, Gordon MN, McGowan E, et al. Accelerated Alzheimer-type phenotype in transgenic mice carrying both mutant *amyloid precursor protein* and *presenilin 1* transgenes. Nat Med. 1998;4:97–100.
7 Takeuchi A, Irizarry MC, Duff K, et al. Age-related amyloid β deposition in transgenic mice overexpressing both Alzheimer mutant presenilin 1 and amyloid β precursor protein Swedish mutant is not associated with global neuronal loss. Am J Pathol. 2000;157:331–339.
8 Jantzen PT, Connor KE, DiCarlo G, et al. Microglial activation and β-amyloid deposit reduction caused by a nitric oxide-releasing nonsteroidal anti-inflammatory drug in amyloid precursor protein plus presenilin-1 transgenic mice. J Neurosci. 2002;22:2246–2254.
9 Kreutzberg GW. Microglia: a sensor for pathological events in the CNS. Trends Neurosci. 1996;19:312–318.
10 Wegiel J, Wisniewski HM. The complex of microglial cells and amyloid star in three-dimensional reconstruction. Acta Neuropathol. 1990;81:116–124.
11 Stalder M, Phinney A, Probst A, Sommer B, Staufenbiel M, Jucker M. Association of microglia with amyloid plaques in brains of APP23 transgenic mice. Am J Pathol. 1999;154:1673–1684.
12 El Khoury J, Hickman SE, Thomas CA, Cao L, Silverstein SC, Loike JD. Scavenger receptor-mediated adhesion of microglia to β-amyloid fibrils. Nature. 1996;382:716–719.
13 Christie RH, Freeman M, Hyman BT. Expression of the macrophage scavenger receptor, a multifunctional lipoprotein receptor, in microglia associated with senile plaques in Alzheimer's disease. Am J Pathol. 1996;148:399–403.
14 Paresce DM, Ghosh RN, Maxfield FR. Microglial cells inter-

nalize aggregates of the Alzheimer's disease amyloid β-protein via a scavenger receptor. Neuron. 1996;17:553–565.
15 Schenk D. Amyloid-β immunotherapy for Alzheimer's disease: the end of the beginning. Nat Rev Neurosci. 2002;3:824–828.
16 Bard F, Cannon C, Barbour R, et al. Peripherally administered antibodies against amyloid β-peptide enter the central nervous system and reduce pathology in a mouse model of Alzheimer disease. Nat Med. 2000;6:916–919.
17 DeMattos RB, Bales KR, Cummins DJ, Paul SM, Holtzman DM. Brain to plasma amyloid-β efflux: a measure of brain amyloid burden in a mouse model of Alzheimer's disease. Science. 2002;295:2264–2267.
18 Wyss-Coray T, Lin C, Yan F, et al. TGF-β1 promotes microglial amyloid-β clearance and reduces plaque burden in transgenic mice. Nat Med. 2001;7:612–618.
19 Kakimura J, Kitamura Y, Taniguchi T, Shimohama S, Gebicke-Haerter PJ. BiP/GRP78-induced production of cytokines and uptake of amyloid-β(1 – 42) peptide in microglia. Biochem Biophys Res Commun. 2001;281:6–10.
20 Kakimura J, Kitamura Y, Takata K, et al. Microglial activation and amyloid-β clearance induced by exogenous heat-shock proteins [Summary]. FASEB J (February 25, 2002) 10.1096/fj.01-0530fje. FASEB J. 2002;16:601–603.
21 Greenberg S. Signal transduction of phagocytosis. Trends Cell Biol. 1995;5:93–99.
22 Ohsawa K, Imai Y, Kanazawa H, Sasaki Y, Kohsaka S. Involvement of Iba1 in membrane ruffling and phagocytosis of macrophages/microglia. J Cell Sci. 2000;113:3073–3084.
23 Hall A. Rho GTPases, the actin cytoskeleton. Science. 1998;279:509–514.
24 Miki H, Sasaki T, Takai Y, Takenawa T. Induction of filopodium formation by a WASP-related actin-depolymerizing protein N-WASP. Nature. 1998;391:93–96.
25 Miki H, Yamaguchi H, Suetsugu S, Takenawa T. IRSp53 is an essential intermediate between Rac and WAVE in the regulation of membrane ruffling. Nature. 2000;408:732–735.
26 Takenawa T, Miki H. WASP and WAVE family proteins: key molecules for rapid rearrangement of cortical actin filaments and cell movement. J Cell Sci. 2001;114:1801–1809.
27 Fukuoka M, Suetsugu S, Miki H, Fukami K, Endo T, Takenawa T. A novel Neural Wiskott-Aldrich syndrome protein (N-WASP) binding protein, WISH, induces Arp2/3 complex activation independent of Cdc42. J Cell Biol. 2001;152:471–482.
28 Fukuoka M, Miki H, Takenawa T. Identification of N-WASP homologs in human and rat brain. Gene. 1997;196:43–48.
29 Kitamura Y, Taniguchi T, Kimura H, Nomura Y, Gebicke-Haerter PJ. Interleukin-4-inhibited mRNA expression in mixed rat glial and in isolated microglial cultures. J Neuroimmunol. 2000;106:95–104.
30 Kaneko I, Tutumi S. Matters arising: conformations of β-amyloid in solution. J Neurochem. 1997;68:438–439.
31 Kitamura Y, Ishida Y, Takata K, et al. Hyperbilirubinemia protects against focal ischemia in rats. J Neurosci Res. 2003;71:544–550.
32 Miura N, Asano A. Synergistic effect of colchicine and cytochalasin D on phagocytosis by peritoneal macrophages. Nature. 1976;261:319–321.
33 Miki H, Miura K, Takenawa T. N-WASP, a novel actin-depolymerizing protein, regulates the cortical cytoskeletal rearrangement in a PIP2-dependent manner downstream of tyrosine kinases. EMBO J. 1996;15:5326–5335.
34 Miki H, Suetsugu S, Takenawa T. WAVE, a novel WASP-family protein involved in actin reorganization induced by Rac. EMBO J. 1998;17:6932–6941.
35 Allen WE, Jones GE, Pollard JW, Ridley AJ. Rho, Rac and Cdc42 regulate actin organization and cell adhesion in macrophages. J Cell Sci. 1997;110:707–720.
36 Nobes CD, Hall A. Rho, Rac and Cdc42 GTPases regulate the assembly of multimolecular focal complexes associated with actin stress fibers, lamellipodia, and filopodia. Cell. 1995;81:53–62.
37 Senior K. Dosing in phase II trial of Alzheimer's vaccine suspended. Lancet Neurol. 2002;1:3.
38 Kitamura Y, Nomura. Stress proteins and glial functions: possible therapeutic targets for neurodegenerative disorders. Pharmacol Ther. 2003;97:35–53.